Submitted: 02 December, 2023 Accepted: 11 January, 2024 Online Published: 30 August, 2024 DOI:10.22514/jomh.2024.136

ORIGINAL RESEARCH

JOMH Journal of Men's Health

The value of ^{18}F-PSMA-1007 PET/CT in preoperative evaluation of prostate cancer within PSA gray area

Shuying Bian[1], Meihao Wang[1], Fei Yao[1], Dongqin Zhu[2], Kehua Pan[1], Yunjun Yang[2], Kun Tang[2], Weifeng Hong[3], Xiaowei Ji[2,*]

[1]The Department of Radiology, The First Affiliated Hospital of Wenzhou Medical University, 325000 Wenzhou, Zhejiang, China
[2]The Department of Nuclear Medicine, The First Affiliated Hospital of Wenzhou Medical University, 325000 Wenzhou, Zhejiang, China
[3]The Department of Radiology, The People's Hospital of Yuhuan, 317600 Yuhuan, Zhejiang, China

***Correspondence**
jixiaowei@wmu.edu.cn
(Xiaowei Ji)

Abstract

^{18}F-prostate-specific membrane antigen (PSMA)-1007 positron emission tomography/computed tomograpy (PET/CT) had been increasingly significant in detecting prostate cancer. This study was aimed to assess the usefulness of ^{18}F-PSMA-1007 PET/CT in preoperative evaluation of prostate cancer for the cases with serum total prostate-specific antigen (tPSA) levels between 4 and 10 ng/mL, referred as the PSA gray area. A total of 117 prostate cancer patients in PSA gray area were retrospectively analyzed in the period between March 2019 and December 2022. The independent predictors of extraprostatic extension (EPE) were identified via the Univariate and multivariate analyses. The maximum standardized uptake value (SUVmax) was the only independent predictor of EPE (odds ratio (OR), 1.114; 95% confidence interval (CI), 1.040–1.194; p = 0.002). The predicted model's area under receiver-operating characteristic curves was 75.4%. The sensitivity, specificity and accuracy of ^{18}F-PSMA-1007 PET/CT were calculated for diagnosing the regional lymph node and bone metastases, and obtained as 85.71%, 99.20%, 99.05% and 100%, 97.35%, 99.15%, respectively. In conclusion, SUVmax as compared to the clinical parameters had higher predictive value for EPE in prostate cancer patients within PSA gray area. ^{18}F-PSMA-1007 PET/CT had thus the satisfactory evaluation efficacy for diagnosing the regional lymph node and bone metastases.

Keywords

Prostate cancer; Positron emission tomography; ^{18}F-prostate-specific membrane antigen; Prostate-specific antigen gray area; Stage

1. Introduction

Prostate cancer (PCa) has the highest occurrence rates among the male cancers in 104 out of 185 countries [1]. It is a malignancy affecting the male urinary system. PCa holds sixth position in China regarding the male cancer-related mortality. It has relatively lower incidence than that in Western nations. However, PCa has started affecting the younger patients because of lifestyle changes [2].

PCa lacks symptoms at the earlier stage which causes difficulties in early PCa management. The European Association of Urology acknowledges serum prostate-specific antigen (PSA) as PCa detection biomarker. The tPSA levels are correlated with PCa diagnosis. The tPSA levels exceeding 10 ng/mL strongly hint cancer. However, it is important whether to diagnose and stage PCa in the "gray area" of tPSA levels between 4.0 ng/mL and 10.0 ng/mL [3–5]. PSA screening must thus be accompanied by imaging examinations to accurately diagnose PCa [6].

Bone scintigraphy (BS), magnetic resonance imaging (MRI), and computed tomography (CT) can assist in evaluating the high-risk PCa cases [7]. However, assessing the invasiveness of PCa in PSA gray area is challenging because most cases are of low-grade malignancies [7]. The prostate-specific membrane antigen (PSMA) PET/CT is a sensitive imaging tool to accurately reflect the histopathology and metastatic disease compared to the traditional methods. It is applicable even to the patients with low PSA levels [8–11]. The membrane-bound enzyme PSMA is lowly expressed in benign prostate tissues and highly in prostate cancer epithelial cells [12]. ^{18}F-PSMA-1007 PET/CT has been excellent in recognizing lymph node and bone metastases [13, 14]. Moreover, the European Association of Urology recommend this examination for PCa patients at clinical stage of T3 or higher, indicating extraprostatic extension (EPE). PET/CT images are visually analyzed. Moreover, the maximum standardized uptake value (SUVmax) as a semi-quantitative evaluation of PSMA expression is obtained from PET/CT, being in line with the European Association of Nuclear Medicine standardized reporting guidelines [15]. However, few studies have investigated the application of ^{18}F-PSMA-1007 PET/CT in the PSA gray area. Purpose of this study was thus to evaluate the significance of ^{18}F-PSMA-1007 PET/CT in preoperative assessment of PCa patients in the PSA gray

area.

2. Material and methods

2.1 Patients

A total of 418 patients undergone ^{18}F-PSMA-1007 PET/CT at our hospital between March 2019 and December 2022 were initially enrolled. The patients had undertaken radical prostatectomy (RP) and pelvic lymph node dissection (PLND) with histopathologically confirmed PCa. After screening, 117 patients were included in this study (**Supplementary Fig. 1a**). The exclusion criteria were as follows: (1) tPSA levels outside the gray area, (2) history of other malignancies, (3) history of local or systemic treatments before ^{18}F-PSMA-1007 PET/CT evaluation, and (4) incomplete clinical information or unclear images. The "gray area" in this study referred to the tPSA levels between 4 ng/mL and 10 ng/mL.

2.2 ^{18}F-PSMA-1007 PET/CT image scanning

PET/CT (Gemini 64 TF, Philips Medical Systems, Best, The Netherlands) was employed to scan every patient from skull to the middle of thigh. Scans were carried out ~90 min after the intravenous injection of 4.0 MBq/kg ^{18}F-PSMA-1007 (mean ± standard deviation dose: 282.94 ± 34.48 MBq). The following parameters were set for a low-dose CT scan: 140 Kvp tube voltage, 110 mA tube current, 64 × 0.625 mm detector collimation, 0.829 pitch, 0.5 s tube rotation speed, 5 mm section thickness, and 2.5 mm reconstruction thickness. A PET scan was conducted by matching the CT section thickness. Images were acquired in three-dimensional mode with parameters of 576 mm field view, 144 × 144 matrix, and 5 mm slice thickness and interval.

2.3 ^{18}F-PSMA-1007 PET/CT image analysis

Images were analysed by a workstation (EBW3.0, Philips). The images were interpreted regarding the primary prostate tumor, pelvic lymph node metastasis and bone metastasis. Tumors were considered positive with the tracer uptake being higher than normal prostate tissue, and the tumor SUVmax was recorded. Metastases was suspected if any lymph node or bone lesion had higher tracer accumulation than the surrounding background [16]. According to the anatomical location, all positive lymph nodes on PET/CT were divided into the areas including left/right external and internal iliac, and left/right obturator areas. This interpretation criterion was consistent with the literature [15, 17]. The images were jointly analyzed by physician and deputy chief physician. They were the nuclear medicine specialists with ten years of experience. Any disagreement was resolved by consensus.

2.4 Collection of clinical and imaging parameters

Clinical parameters including age, serum PSA level, prostate volume (PV), and prostate-specific antigen density (PSAD) were collected from the hospital database. Serum PSA levels were recorded at the initial diagnosis. PV was calculated as: volume = anteroposterior diameter × left-right diameter × vertical diameter × $\pi/6$. Diameters were measured at the significant and clearest sections of prostate on CT images [18]. PSAD was calculated as: PSAD = PSA/PV. SUVmax was measured in the region of the highest tracer uptake among primary prostate lesions present in images.

2.5 Comparison between histopathology and PET/CT

Histopathological examinations were conducted for all the patients as per routine, and data were extracted from the pathology reports of RP specimens. The data pertaining to tumor stage, International Society of Urological Pathology (ISUP) grade, and presence of lymph nodes were recorded. PET/CT diagnostic potential was assessed by comparing the imaging and histopathological results. Tumor node metastasis (TNM) staging was analyzed and compared to obtain accurate results (**Supplementary Fig. 1b**). Histopathological analysis was taken as the reference for EPE and regional lymph node metastasis. Bone metastasis was determined via the clinical follow-up.

2.6 Statistical analysis

SPSS software (version 25.0, IBM, Armonk, NY, USA) was employed for the statistical analyses. Normal distribution variables are presented as mean ± standard deviation, while skewed variables as median (range). Categorical variables are expressed as the number of occurrences (n) and frequency (%). These variables were analyzed by employing Student's *t*-test or Mann-Whitney U-test, and chi-square or Fisher's exact test. The independent predictive factors for EPE were identified by Logistic regression analysis. The predictive models were established by receiver operating characteristic (ROC) curve and the area under ROC curve (AUC) with different parameters. The differences between ROC curves were evaluated by Delong's test. Sensitivity (SE), specificity (SP), positive predictive value (PPV), and negative predictive value (NPV) were calculated to evaluate the ^{18}F-PSMA-1007 PET/CT performance in diagnosing lymph node and bone metastases. Statistical significance was set at $p < 0.05$.

3. Results

3.1 Patients

Patient characteristics were given in Table 1. The study included 117 PCa patients with median age of 69 and median tPSA value of 6.72 ng/mL. ISUP grade of the patients ranged from I to V. The median SUVmax of EPE patients was 11.55 (4.50–66.20) compared to that of 8.70 (4.30–31.80) in non-EPE patients ($p < 0.001$).

3.2 Pathological T stage

3.2.1 Clinical and imaging characteristics

^{18}F-PSMA-1007 PET/CT images of 117 patients depicted different radioactive concentrations in the prostate (Fig. 1). The distribution of T stages for patients undergone RP and pathological specimens available for evaluation was as follows: T2 (54.70%), T3a (29.91%), T3b (12.82%) and T4 (2.56%)

TABLE 1. Characteristics of the patient population.

	Total patients (n = 117)	EPE patients (n = 52)	Non-EPE patients (n = 65)	*p* value
Age (yr)				
Median (range)	69.00 (43.00–83.00)	68.50 (54.00–83.00)	69.00 (43.00–81.00)	0.976
tPSA (ng/mL)				
Median (range)	6.72 (4.03–9.97)	6.83 (4.03–9.72)	6.70 (4.05–9.97)	0.750
fPSA (ng/mL)				
Median (range)	0.83 (0.22–2.61)	0.89 (0.26–2.61)	0.74 (0.22–1.98)	0.171
t/fPSA (ng/mL)				
Median (range)	0.11 (0.04–0.36)	0.11 (0.04–0.34)	0.11 (0.04–0.34)	0.249
PV (mL)				
Median (range)	35.88 (12.75–79.67)	33.71 (12.75–79.67)	37.70 (20.02–79.61)	0.183
PSAD (ng/mL^2)				
Median (range)	0.18 (0.08–0.46)	0.19 (0.09–0.46)	0.17 (0.08–0.39)	0.200
SUVmax				
Median (range)	9.50 (4.30–66.20)	11.55 (4.50–66.20)	8.70 (4.30–31.80)	<0.001
ISUP, n (%)				
I	5 (4.27%)	1 (1.92%)	4 (6.15%)	
II	45 (38.46%)	13 (25.00%)	32 (49.23%)	
III	45 (38.46%)	25 (48.08%)	20 (30.77%)	0.003
IV	8 (6.84%)	4 (7.69%)	4 (6.15%)	
V	14 (11.97%)	9 (17.31%)	5 (7.70%)	
Clinical TNM stage on ^{18}F-PSMA-1007 PET/CT				
T stage				
T2	67 (57.26%)	8 (15.38%)	59 (90.77%)	
T3a	32 (27.35%)	30 (57.69%)	2 (3.08%)	<0.001
T3b	13 (11.11%)	10 (19.23%)	3 (4.62%)	
T4	5 (4.28%)	4 (7.70%)	1 (1.53%)	
N stage				
N0	110 (94.02%)	45 (86.54%)	65 (100.00%)	0.002
N1	7 (5.98%)	7 (13.46%)	0 (0.00%)	
M stage				
M0	109 (93.16%)	47 (90.38%)	62 (95.38%)	0.487
M1	8 (6.84%)	5 (9.62%)	3 (4.62%)	
Pathological TNM stage				
T stage				
T2	64 (54.70%)	0 (0.00%)	64 (98.46%)	
T3a	35 (29.91%)	34 (65.38%)	1 (1.54%)	<0.001
T3b	15 (12.82%)	15 (28.85%)	0 (0.00%)	
T4	3 (2.56%)	3 (5.77%)	0 (0.00%)	
N stage				
N0	113 (96.58%)	48 (92.31%)	65 (100.00%)	0.023
N1	4 (3.42%)	4 (7.69%)	0 (0.00%)	
M stage*				
M0	110 (94.02%)	47 (90.38%)	63 (96.92%)	0.931
M1	7 (5.98%)	5 (9.62%)	2 (3.08%)	

M stage: M stage is not determined by bone biopsy, but by clinical follow-up.*

EPE: extraprostatic extension; PSA: prostate-specific antigen; PV: prostate volume; SUVmax: maximum standardized uptake value; ISUP: international society of urological pathology; PSMA: prostate-specific membrane antigen; CT: computed tomography; PSAD: prostate-specific antigen density; TNM: tumor node metastasis; PET: positron emission tomography.

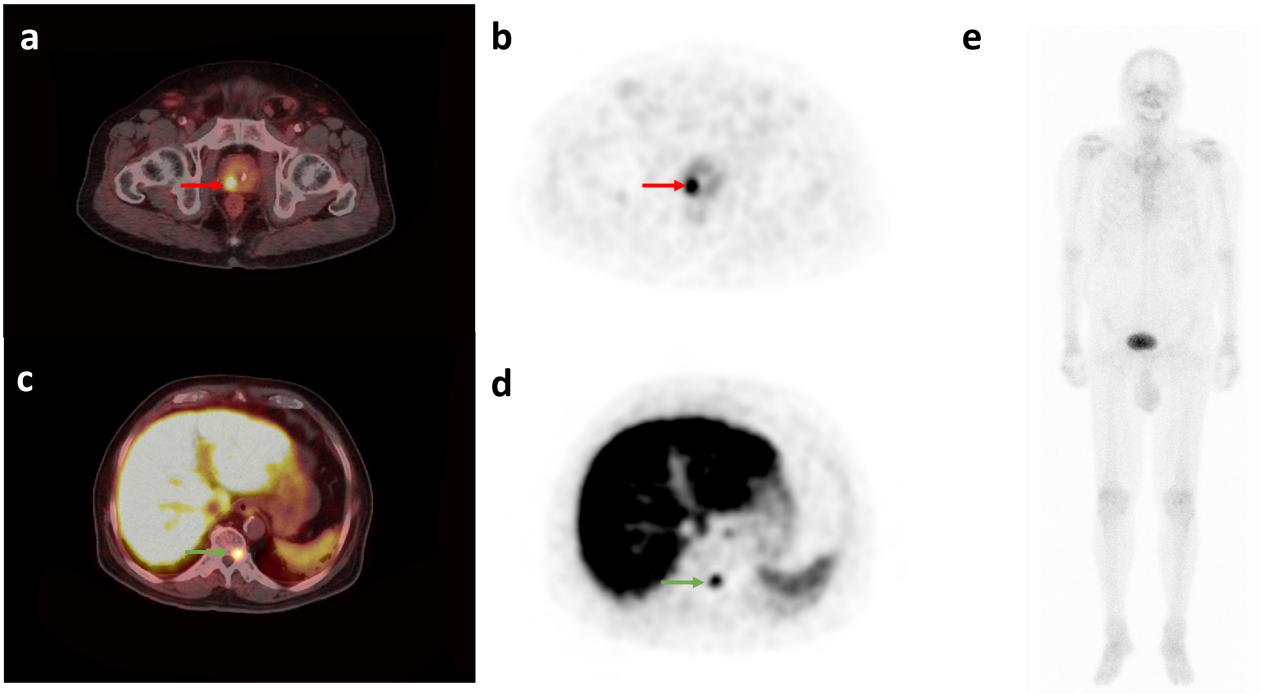

FIGURE 1. A patient of bone metastasis with PSA 5.78 ng/mL, GS 4 + 4. (a,b) Abnormally increased PSMA uptake in right glands (red arrow), SUVmax is 28.0. (c,d) The T10 vertebral body with increased PSMA uptake (green arrow), SUVmax is 11.5. (e) No concentration of bone on ^{99}mTc-MDP SPECT. (a,c) fused PET/CT; (b,d) axial PET; (e) ^{99}mTc-MDP SPECT.

(Table 1).

3.2.2 EPE prediction by logistic regression analysis

Table 1 showed the details of EPE of patients. PV, PSAD and tPSA did not change much ($p > 0.05$; Fig. 2a–d), however, significant difference was found in SUVmax between EPE and Non-EPE ($p < 0.001$). EPE risk was positively correlated with SUVmax as depicted in univariate logistic analysis (odds ratio (OR), 1.097; 95% confidence interval (CI), 1.032–1.167; $p = 0.003$; Table 2). SUVmax was the only independent predictor of EPE as found in multivariate logistic regression (OR, 1.114; 95% CI, 1.040–1.194; $p = 0.002$; Table 2).

3.2.3 Comparing tPSA, SUVmax and combined model by ROC curves for predicting EPE

ROC curves showed the AUC for tPSA as 0.52 (95% CI: 0.42–0.61). The AUC for SUVmax and combined model were 0.71 (95% CI: 0.62–0.79) and 0.75 (95% CI: 0.67–0.83), respectively, both being higher than that for tPSA ($p < 0.05$; Fig. 3a). SUVmax exhibited the best predictive value compared to clinical parameters.

3.3 Lymph node metastasis

^{18}F-PSMA-1007 PET/CT revealed abnormal pelvic lymph node uptake in 7 of 117 patients. **Supplementary Table 1** provided the characteristics of patients with pelvic lymph node metastasis. RP and PLND were conducted based on the patients' images where 634 lymph nodes were examined. Seven patients had pelvic metastasis with diameter of 0.2 cm–2.1 cm. SE, SP, PPV, NPV and accuracy (ACC) were 100%, 97.35%, 57.14%, 100% and 97.44%, respectively. Seven of 634 examined lymph nodes were positive. The median SUVmax of true-positive lymph node metastasis (LNMs) was larger (9.03 ± 6.17) than that of false-positive LNMs (5.20 ± 1.18). SE, SP, PPV, NPV and ACC at PET/CT were 85.71%, 99.20%, 54.55%, 99.84% and 99.05%, respectively (Table 3).

3.4 Bone metastasis

The median follow-up time for evaluating bone metastases was 18 months (8–34 months). The common sites of bone lesions in this study were pelvis and spine. Seven patients were identified with PCa having bone metastases on PET/CT images. Six had different degrees of metastatic progression in the clinical follow-up while one had no disease progression. **Supplementary Table 2** showed the patients' details. Three patients underwent PET/CT because of the bone pain where bone metastasis and primary PCa lesion were found. ^{99}mTc-methylene diphosphonic acid (MDP) single-photon emission computed tomography (SPECT) demonstrated metastasis in two patients as depicted by PET/CT, while the other one had bone pain in the clinical follow-up. The treatment regimen was affected as the staging changed from M0 to M1 in above patients (Fig. 1). SE, SP, PPV, NPV and ACC at PET/CT were 100%, 97.35%, 85.71%, 100% and 99.15%, respectively (Table 4).

3.5 Associating SUVmax with ISUP

No significant difference was found in PV, PSAD, or tPSA ($p > 0.05$; Fig. 2e–h), while it was there in SUVmax between ISUP <4 and ISUP ≥4 ($p < 0.001$). The risk of ISUP ≥4 was positively correlated with SUVmax as found in univariate

TABLE 2. Univariate and multivariate logistic regression for EPE predictors.

Variable	Univariate logistic regression				Multivariate logistic regression			
	OR	95% CI	*p* value	Predictive accuracy, %	OR	95% CI	*p* value	Predictive accuracy, %
SUVmax	1.097	1.032–1.167	0.003	71.0%	1.114	1.040–1.194	0.002	
Age	1.009	0.954–1.067	0.758	49.8%	0.982	0.920–1.049	0.591	
fPSA	1.695	0.743–3.864	0.210	57.4%	3.670	0.420–4.699	0.116	
tPSA	1.037	0.829–1.298	0.749	51.7%	0.624	0.307–1.268	0.193	75.4%
f/tPSA	1.313	0.056–3.101	0.252	56.2%	0.000	0.000–9.667	0.253	
PV	0.983	0.957–1.010	0.221	57.2%	0.985	0.919–1.055	0.666	
PSAD	2.636	0.333–2.880	0.142	56.9%	1.812	0.000–2.160	0.668	

EPE: extraprostatic extension; SUVmax: maximum standardized uptake value; PSA: prostate-specific antigen; PV: prostate volume; OR: odds ratio; CI: confidence interval; PSAD: prostate-specific antigen density.

TABLE 3. Accuracy of ^{18}F-PSMA-PET/CT for N stage.

For RP patients' analysis			
n = 117	HP+ (n = 4)	HP– (n = 113)	
PET+ (n = 7)	4	3	PPV 57.14%
PET– (n = 110)	0	110	NPV 100%
	SE 100%	SP 97.35%	ACC 97.44%
For PLND nodes analysis of RP patients			
n = 634	HP+ (n = 7)	HP– (n = 627)	
PET+ (n = 11)	6	5	PPV 54.55%
PET– (n = 623)	1	622	NPV 99.84%
	SE 85.71%	SP 99.20%	ACC 99.05%

A total of 117 RP patients with PLND were analyzed by histopathology (HP). Sensitivity (SE), specificity (SP), positive predictive value (PPV), negative predictive value (NPV), and accuracy (ACC) in detecting PCa were given in percent.
RP: radical prostatectomy; PLND: pelvic lymph node dissection; PET: positron emission tomography.

TABLE 4. Accuracy of ^{18}F-PSMA-PET/CT for M stage.

n = 117	Clinical follow up+ (n = 6)	Clinical follow up– (n = 111)	
PET+ (n = 7)	6	1	PPV 85.71%
PET– (n = 110)	0	110	NPV 100.00%
	SE 100%	SP 97.35%	ACC 99.15%

A total of 117 patients for M stage were analyzed by clinical follow-up. Sensitivity (SE), specificity (SP), positive predictive value (PPV), negative predictive value (NPV), and accuracy (ACC) in detecting PCa were given in percent. PET: positron emission tomography.

logistic analysis (OR, 1.126; 95% CI, 1.055–1.202; $p < 0.001$). SUVmax was the only independent predictor of ISUP $\geq$4 as revealed in multivariate logistic regression (OR, 1.136; 95% CI, 1.057–1.221; $p = 0.001$; **Supplementary Table 3**. ROC curves exhibited the AUC for tPSA as 0.55 (95% CI: 0.45–0.64). AUC for SUVmax and combined model were 0.78 (95% CI: 0.69–0.85) and 0.81 (95% CI: 0.72–0.87), both being higher than tPSA ($p < 0.05$; Fig. 3b). SUVmax depicted the best predictive value compared to the clinical parameters.

4. Discussion

Evaluation of PCa based on the PSA gray area was challenging. This study was aimed to evaluate the value of ^{18}F-PSMA-1007 PET/CT in PSA gray area. The results demonstrated that PET/CT could predict EPE in patients within PSA gray area, and surpassed the performance of clinical parameters alone. Furthermore, PET/CT was efficient in detecting regional lymph nodes and bone metastases.

Histopathology was the standard criterion for PCa staging, however the detection rates of current detection methods were low in patients with lower PSA levels. ^{18}F-PSMA-1007 PET/CT as a new imaging method had relatively little research conducted.

The concentration of lesions was detected in all patients of this study. Wang *et al.* [19] concluded that the PSA levels in biochemical recurrence were lower than those in initial diagnosis, however ^{18}F-PSMA-1007 PET/CT could still detect the lesion. In contrast, the PSA gray areas of included patients were the first ones not diagnosed with biochemical recurrence, nonetheless, the results herein showed high accuracy. The histopathological results were staged wherein more than half patients were of T2 stage. This could be attributed to the relatively low PSA levels in most patients. The relationship between the T stage and various parameters was further studied. SUVmax was the only independent predictor of EPE at the tPSA of 4 ng/mL–10 ng/mL. SUVmax (AUC = 0.71) and the combined model (AUC = 0.75) had better predictive value than tPSA (AUC = 0.52; $p < 0.05$). This confirmed the previous findings [20, 21] that the semi quantitative analysis indicators of PSMA PET/CT imaging including SUVmax,

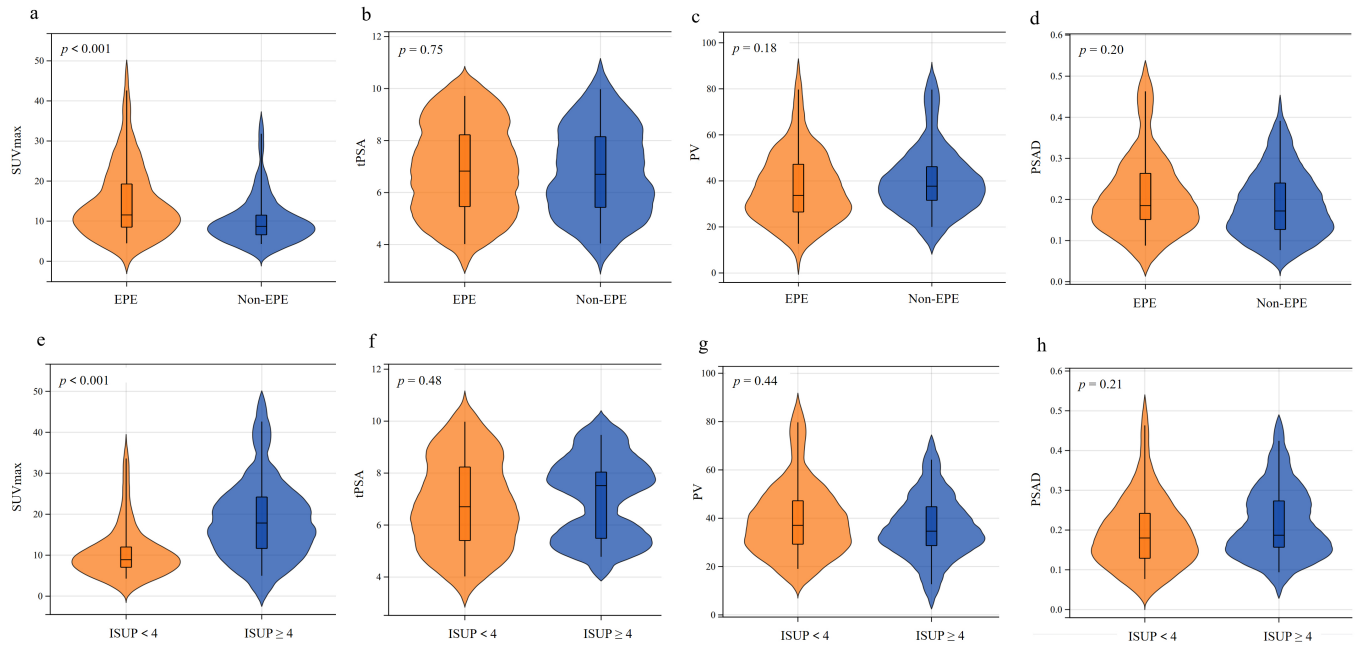

FIGURE 2. The differences between EPE and Non-EPE. (a–d) suggest differences in variables between EPE and Non-EPE. (e–h) suggest differences in variables between ISUP <4 and ISUP ≥4. SUVmax: maximum standardized uptake value; PSA: prostate-specific antigen; EPE: extraprostatic extension; PV: prostate volume; ISUP: international society of urological pathology; PSAD: prostate-specific antigen density.

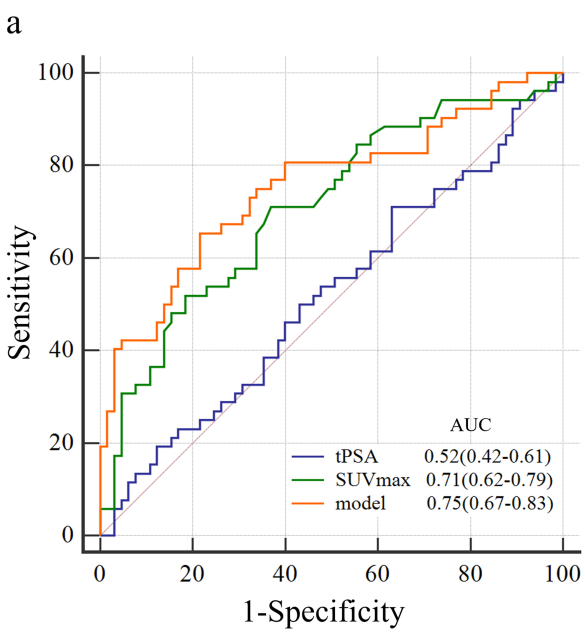

Comparison	*p* value
tPSA *vs* SUVmax	0.005
tPSA *vs* model	< 0.001
SUVmax *vs* model	0.300

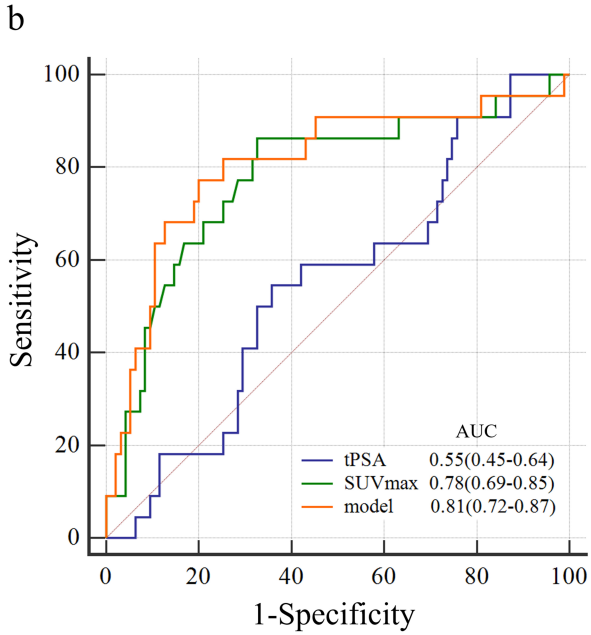

Comparison	*p* value
tPSA *vs* SUVmax	0.006
tPSA *vs* model	0.002
SUVmax *vs* model	0.194

FIGURE 3. Comparison of ROC curves. (a) ROC curves comparing tPSA, SUVmax and combined model to predict EPE. AUC to predict EPE was 0.52 for tPSA, 0.71 for SUVmax and 0.75 for combined model. (b) ROC curves comparing tPSA, SUVmax and combined model to predict ISUP ≥4. AUC to predict ISUP ≥4 was 0.55 for tPSA, 0.78 for SUVmax and 0.81 for combined model. tPSA: total prostate-specific antigen; SUVmax: maximum standardized uptake value; AUC: area under ROC curve.

could predict the risk stratification of prostate cancer. If SUVmax of the prostate lesions in PSMA PET/CT was higher than expected, the treatment plan could be adjusted by performing extended PLND or androgen deprivation therapy in suspected EPE patients. SUVmax was thus proved as the only independent predictor of ISUP ≥4 (OR, 1.136; 95% CI, 1.057–1.221; p = 0.001). ISUP ≥4 indicated a high PCa risk. The biopsy ISUP was not always consistent with the pathological ISUP. Therefore, SUVmax might predict the pathological ISUP more reliably compared to the biopsy ISUP and the other less sensitive clinical variables. The patients with high SUVmax might skip the biopsy and directly undergo the next treatment steps. In this study, the multivariate analyses revealed that none of the clinical parameters were independent predictors of PSA range. Studies [22–24] had reported that the clinical parameters including age, PV and PSAD were not the predictors in these patients. PCa patients usually had prostate hyperplasia. The changes in prostate size caused by hyperplasia might affect PSAD in the males with tPSA levels of 4 ng/mL–10 ng/mL. The predictive value of these clinical indicators remained controversial within PSA gray areas. The racial differences and sample selection biases might be responsible for this result.

Some patients did not undergo PLND because of the low preoperative risk of lymph node involvement. The specificity and accuracy of ^{18}F-PSMA-1007 PET/CT in detecting lymph node metastases were satisfactory in this study. Previous investigations proved that PET/CT had greater specificity for LNM staging of intermediate-risk or high-risk PCa [25]. This study further depicted that ^{18}F-PSMA-1007 PET/CT was accurate for the LNM staging in PCa patients and with low PSA values. Researchers using histopathology for the validation had demonstrated that PET/CT possessed sufficient diagnostic value in LNM staging by employing ^{68}Ga-PSMA as a tracer. ^{18}F-PSMA had rarely been studied [21, 26, 27]. A precedent was thus set to prove ^{18}F-PSMA-1007 PET/CT being applicable for lymph node staging.

Distant metastases were important for the prognosis which emphasized clinical importance of their detection. ^{18}F-PSMA-1007 PET/CT showed the diagnostic accuracy of 99.15%, being consistent with the previous studies [28, 29]. Sometimes, the concentration focus on PET/CT could not be observed on ^{99}mTc-MDP SPECT because of the difference in imaging principles of two methods. Bone uptake of ^{99}mTc-MDP was related to the osteoblast activity, vascularization and environmental factors. PCa bone metastasis triggered an osteoblast response and accumulated large amounts of ^{99}mTc-MDP. PSMA PET/CT was more sensitive to detect bone metastases than BS in the patients of PSA <10 ng/mL [30]. There was no concentration of ^{99}mTc-MDP SPECT in the patient whose PSMA PET/CT was positive (Fig. 1). This did not completely rule out the metastasis possibility. A possible reason could be that the follow-up time was not long enough, and focus was not osteogenic. This patient should thus be continued with active treatment because of bone pain symptoms. Early detection of PSMA PET/CT for bone metastasis could determine the appropriate treatment plan.

This study had several limitations. The selection bias might impact the findings as it was a retrospective study with small sample size and carried out at a single center. Furthermore, bone metastases were not confirmed by histopathology as the confirmatory biopsies were not routinely performed for suggestive bone lesions. Therefore, it was planned to validate these results in a prospective study with multicenter data, and conduct subgroup analysis of different T stages. Furthermore, the follow-up time for the metastatic patients should be prolonged to attain more accurate prognosis. Future studies would focus these areas.

5. Conclusions

This study evaluated the potential of ^{18}F-PSMA-1007 PET/CT in preoperative evaluation of prostate cancer within PSA gray area. It exhibited an excellent diagnostic performance for EPE, lymph node metastasis, and bone metastasis.

ABBREVIATIONS

PSMA, prostate-specific membrane antigen; PET, positron emission tomography; PSA, prostate-specific antigen; RP, radical prostatectomy; PCa, prostate cancer; SUVmax, maximum standardized uptake value; PSAD, prostate-specific antigen density; ISUP, international society of urologic pathology; mpMRI, multiparametric magnetic resonance imaging; CT, computed tomography; BS, bone scintigraphy; ROC, receiver operating characteristic; PLND, pelvic lymph node dissection; TNM, tumor node metastasis; LNM, lymph node metastasis; ACC, accuracy; MDP, methylene diphosphonic acid; SPECT, single-photon emission computed tomography.

AVAILABILITY OF DATA AND MATERIALS

The data presented in this study are available on reasonable request from the corresponding author.

AUTHOR CONTRIBUTIONS

SYB—wrote the original manuscript; MHW and FY—interpreted the data and prepared the tables and figures; KHP and DQZ—acquired the data; YJY—contributed to the conception and design of the study; KT and WFH—contributed to the conception and design of the study; XWJ—revised the manuscript for intellectual content. All authors contributed to editorial changes in the manuscript. All authors read and approved the final manuscript.

ETHICS APPROVAL AND CONSENT TO PARTICIPATE

This retrospective study was approved by the Johns Hopkins Institutional Review Board (KY2022-R012) and carried out in accordance with the Declaration of Helsinki. The patients provided written informed consent to participate in this study.

ACKNOWLEDGMENT

Not applicable.

FUNDING

This research was funded by the Key Laboratory of Intelligent Medical Imaging of Wenzhou (No. 2021HZSY0057), the Taizhou Science and Technology Project (Grant No. 20ywb 156), the Wenzhou Major Program of Science and Technology Innovation (Grant No. ZY2020012) and the Key Laboratory of Novel Nuclide Technologies on Precision Diagnosis and Treatment & Clinical Transformation of Wenzhou City (No. 2023HZSY0012).

CONFLICT OF INTEREST

The authors declare no conflict of interest.

SUPPLEMENTARY MATERIAL

Supplementary material associated with this article can be found, in the online version, at https://oss.jomh.org/files/article/1829450036915650560/attachment/Supplementary%20material.docx.

REFERENCES

[1] Bray F, Ferlay J, Soerjomataram I, Siegel RL, Torre LA, Jemal A. Global cancer statistics 2018: GLOBOCAN estimates of incidence and mortality worldwide for 36 cancers in 185 countries. CA: A Cancer Journal for Clinicians. 2018; 68: 394–424.

[2] Chen W. Cancer statistics: updated cancer burden in China. Chinese Journal of Cancer Research. 2015; 27: 1.

[3] Chen M, Ma T, Li J, Zhang HJ, Li Q, Wang JJ, *et al*. Diagnosis of prostate cancer in patients with prostate-specific antigen (PSA) in the gray area: construction of 2 predictive models. Medical Science Monitor. 2021; 27: e929913.

[4] Gentile F, La Civita E, Della Ventura B, Ferro M, Cennamo M, Bruzzese D, *et al*. A combinatorial neural network analysis reveals a synergistic behaviour of multiparametric magnetic resonance and prostate health index in the identification of clinically significant prostate cancer. Clinical Genitourinary Cancer. 2022; 20: e406–e410.

[5] Gentile F, La Civita E, Ventura BD, Ferro M, Bruzzese D, Crocetto F, *et al*. A neural network model combining [−2] proPSA, freePSA, total PSA, cathepsin D, and thrombospondin-1 showed increased accuracy in the identification of clinically significant prostate cancer. Cancers. 2023; 15: 1355.

[6] Aminsharifi A, Howard L, Wu Y, De Hoedt A, Bailey C, Freedland SJ, *et al*. Prostate specific antigen density as a predictor of clinically significant prostate cancer when the prostate specific antigen is in the diagnostic gray zone: defining the optimum cutoff point stratified by race and body mass index. Journal of Urology. 2018; 200: 758–766.

[7] Mottet N, van den Bergh RCN, Briers E, Van den Broeck T, Cumberbatch MG, De Santis M, *et al*. EAU-EANM-ESTRO-ESUR-SIOG guidelines on prostate cancer-2020 update. Part 1: screening, diagnosis, and local treatment with curative intent. European Urology. 2021; 79: 243–262.

[8] Donato P, Roberts M, Morton A, Kyle S, Coughlin G, Esler R, *et al*. Improved specificity with Ga PSMA PET/CT to detect clinically significant lesions "invisible" on multiparametric MRI of the prostate: a single institution comparative analysis with radical prostatectomy histology. European Journal of Nuclear Medicine and Molecular Imaging. 2019; 46: 20–30.

[9] de Feria Cardet RE, Hofman MS, Segard T, Yim J, Williams S, Francis RJ, *et al*. Is prostate-specific membrane antigen positron emission tomography/computed tomography imaging cost-effective in prostate cancer: an analysis informed by the proPSMA trial. European Urology. 2021; 79: 413–418.

[10] Li Y, Han D, Wu P, Ren J, Ma S, Zhang J, *et al*. Comparison of ^{68}Ga-PSMA-617 PET/CT with mpMRI for the detection of PCa in patients with a PSA level of 4–20 ng/mL before the initial biopsy. Scientific Reports. 2020; 10: 10963.

[11] Jochumsen MR, Bouchelouche K. PSMA PET/CT for primary staging of prostate cancer—an updated overview. Seminars in Nuclear Medicine. 2024; 54: 39–45.

[12] Ruigrok EAM, van Weerden WM, Nonnekens J, de Jong M. The future of PSMA-targeted radionuclide therapy: an overview of recent preclinical research. Pharmaceutics. 2019; 11: 560.

[13] Woo S, Ghafoor S, Becker AS, Han S, Wibmer AG, Hricak H, *et al*. Prostate-specific membrane antigen positron emission tomography (PSMA-PET) for local staging of prostate cancer: a systematic review and meta-analysis. European Journal of Hybrid Imaging. 2020; 4: 16.

[14] Ingvar J, Hvittfeldt E, Trägårdh E, Simoulis A, Bjartell A. Assessing the accuracy of [^{18}F]PSMA-1007 PET/CT for primary staging of lymph node metastases in intermediate- and high-risk prostate cancer patients. EJNMMI Research. 2022; 12: 48.

[15] Ceci F, Oprea-Lager DE, Emmett L, Adam JA, Bomanji J, Czernin J, *et al*. E-PSMA: the EANM standardized reporting guidelines v1.0 for PSMA-PET. European Journal of Nuclear Medicine and Molecular Imaging. 2021; 48: 1626–1638.

[16] Fanti S, Goffin K, Hadaschik BA, Herrmann K, Maurer T, MacLennan S *et al*. Consensus statements on PSMA PET/CT response assessment criteria in prostate cancer. European Journal of Nuclear Medicine and Molecular Imaging. 2021; 48: 469–476.

[17] van Leeuwen PJ, Emmett L, Ho B, Delprado W, Ting F, Nguyen Q, *et al*. Prospective evaluation of 68Gallium-prostate-specific membrane antigen positron emission tomography/computed tomography for preoperative lymph node staging in prostate cancer. BJU International. 2017; 119: 209–215.

[18] Marin L, Ezziane M, Comperat E, Mozer P, Cancel-Tassin G, Coté JF, *et al*. Comparison of semi-automated and manual methods to measure the volume of prostate cancer on magnetic resonance imaging. Diagnostic and Interventional Imaging. 2017; 98: 423–428.

[19] Wang R, Shen G, Huang M, Tian R. The diagnostic role of ^{18}F-choline, ^{18}F-fluciclovine and ^{18}F-PSMA PET/CT in the detection of prostate cancer with biochemical recurrence: a meta-analysis. Frontiers in Oncology. 2021; 11: 684629.

[20] Bodar YJL, Veerman H, Meijer D, de Bie K, van Leeuwen PJ, Donswijk ML, *et al*. Standardised uptake values as determined on prostate-specific membrane antigen positron emission tomography/computed tomography is associated with oncological outcomes in patients with prostate cancer. BJU International. 2022; 129: 768–776.

[21] Hoffmann MA, Müller-Hübenthal J, Rosar F, Fischer N, von Eyben FE, Buchholz HG, *et al*. Primary staging of prostate cancer patients with [^{18}F]PSMA-1007 PET/CT Compared with [^{68}Ga]Ga-PSMA-11 PET/CT. Journal of Clinical Medicine. 2022; 11: 5064.

[22] Rodríguez Cabello MA, Méndez Rubio S, Platas Sancho A, Carballido Rodríguez J. Diagnostic evaluation and incorporation of PSA density and the prostate imaging and data reporting system (PIRADS) version 2 classification in risk-nomograms for prostate cancer. World Journal of Urology. 2022; 40: 2439–2450.

[23] Wei C, Chen T, Zhang Y, Pan P, Dai G, Yu H, *et al*. Biparametric prostate MRI and clinical indicators predict clinically significant prostate cancer in men with "gray zone" PSA levels. European Journal of Radiology. 2020; 127: 108977.

[24] Xu N, Wu Y, Chen D, Ke Z, Cai H, Wei Y, *et al*. Can prostate imaging reporting and data system version 2 reduce unnecessary prostate biopsies in men with psa levels of 4–10 ng/mL? Journal of Cancer Research and Clinical Oncology. 2018; 144: 987–995.

[25] Campaña J, Bernal P. Prospective comparison of 18F-PSMA-1007 PET/CT, whole-body MRI and CT in primary nodal staging of unfavorable intermediate and high-risk prostate cancer. European Journal of Nuclear Medicine and Molecular Imaging. 2021; 48: 2670–2671.

[26] Onal C, Ozyigit G, Oymak E, Guler OC, Hurmuz P, Tilki B, *et al*. Clinical parameters and nomograms for predicting lymph node metastasis detected with ^{68}Ga-PSMA-PET/CT in prostate cancer patients candidate to definitive radiotherapy. The Prostate. 2021; 81: 648–656.

[27] Franklin A, Yaxley W, Raveenthiran S, Coughlin G, Gianduzzo T, Kua B, *et al*. Histological comparison between predictive value of preoperative 3-T multiparametric MRI and ^{68}Ga-PSMA PET/CT scan for pathological

outcomes at radical prostatectomy and pelvic lymph node dissection for prostate cancer. BJU international. 2021; 127: 71–79.

[28] Donswijk ML, van Leeuwen PJ, Vegt E, Cheung Z, Heijmink SWTPJ, van der Poel HG, *et al*. Clinical impact of PSMA PET/CT in primary prostate cancer compared to conventional nodal and distant staging: a retrospective single center study. BMC Cancer. 2020; 20: 723.

[29] Sachpekidis C, Bäumer P, Kopka K, Hadaschik B, Hohenfellner M, Kopp-Schneider A, *et al*. ^{68}Ga-PSMA PET/CT in the evaluation of bone metastases in prostate cancer. European Journal of Nuclear Medicine and Molecular Imaging. 2018; 45: 904–912.

[30] Chow KM, So WZ, Lee HJ, Lee A, Yap DWT, Takwoingi Y, *et al*. Head-to-head comparison of the diagnostic accuracy of prostate-specific membrane antigen positron emission tomography and conventional imaging modalities for initial staging of intermediate- to high-risk prostate cancer: a systematic review and meta-analysis. European Urology. 2023; 84: 36–48.

How to cite this article: Shuying Bian, Meihao Wang, Fei Yao, Dongqin Zhu, Kehua Pan, Yunjun Yang, *et al*. The value of ^{18}F-PSMA-1007 PET/CT in preoperative evaluation of prostate cancer within PSA gray area. Journal of Men's Health. 2024; 20(8): 109-117. doi: 10.22514/jomh.2024.136.